LEO Charging of the PICASSO Cubesat and Simulation of the Langmuir Probes Operation

Andreas Waets, Fabrice Cipriani, and Sylvain Ranvier

***Abstract*— The sweeping Langmuir probe (SLP) instrument is a payload of the European Space Agency's (ESA) in-orbit demonstrator PicoSatellite for Atmospheric and Space Science Observations (PICASSO) cubesat, measuring the plasma environment in a high-inclination low earth orbit (LEO) orbit. Because of the small size of the spacecraft (0.3 m × 0.1 m × 0.1 m), the spacecraft floating potential can significantly drift when sweeping the probe bias voltage, affecting the current–voltage characteristic from which plasma parameters are retrieved. In LEO, the spacecraft generally encounters a high-density, cold (less than 1 eV) plasma environment, but due to the high orbital inclination, PICASSO passes the auroral regions exposing the spacecraft to precipitating fluxes of hot (several kiloelectron volts) electrons with potentially harmful, high-level spacecraft charging as a result. To investigate the spacecraft charging and the in-orbit operation of the Langmuir probes in both of these regimes, simulations of PICASSO were carried out in Spacecraft Plasma Interaction System (SPIS). The conditions of the LEO plasma and the constraints imposed by the particle-in-cell (PIC) models on the mesh size make this type of plasma simulations a very challenging task.**

***Index Terms*— Aurora, cubesat, Langmuir, LEO, plasma, probe.**

I. Introduction

PICOSATELLITE for Atmospheric and Space Science Observations (PICASSO) is a cubesat-based project initiated by the Royal Belgian Institute for Space Aeronomy (BIRA-IASB) and administered by the European Space Agency (ESA) as an in-orbit demonstrator of scientific applications from low earth orbit (LEO) cubesat platforms [1]. The objective of the PICASSO mission is to demonstrate the capacity of low-cost nanosatellites to perform remote and *in situ* scientific measurements and to bring the instruments and on-board data processing components to high technology readiness levels. The scientific payload of the spacecraft consists of VISION, a tunable spectral imager which will retrieve a vertical ozone profile by observing the earth's atmospheric limb during the orbital solar occultation, and sweeping Langmuir probe (SLP), an upgraded version of the traditional Langmuir probe. The charging behavior of the PICASSO spacecraft is affected by the operation of the SLP instrument due to the biasing of Langmuir probes with respect to the spacecraft electrical ground. In turn, the interpretation of the SLP data will also rely on a numerical model permitting to simulate the probes response to the environment. The simulation of PICASSO charging in an LEO environment and of the current–voltage (I–V) characteristics of the probes using Spacecraft Plasma Interaction System (SPIS) [2] is the primary focus of this paper.

The LEO plasma environment which PICASSO will encounter is described in Section II. In Section III, the PICASSO spacecraft is described along with a detailed overview of the SLP instrument, followed by the results from the SPIS simulations in Section IV, which are further discussed in Section V. Our conclusions are summarized in Section VI.

TABLE I
Expected Plasma Parameters (Adapted From [3])

	Min. ($> 95\%$ probability)	Max. ($> 95\%$ probability)
Plasma density $[m^{-3}]$	10^8 (10^9)	10^{13} (5×10^{12})
Electron temperature $[eV]$	0.05 (0.06)	1 (0.45)
Debye length $[m]$	5.4E-4 (8.2E-4)	0.69 (0.15)

II. LEO Plasma Environment

PICASSO will be launched in an LEO with a current baseline altitude of ∼550 km and an inclination of 98° [3], completing an orbit approximately every 90 min. The Langmuir probe instrument on-board is designed to measure plasma parameters between 400 and 700 km, in case PICASSO is required to operate at an orbital altitude different from the baseline. The spacecraft will fly through the middle and upper layers of the ionosphere where it predominantly encounters high-density, cold plasma. Expected plasma parameter ranges are given in Table I.

Manuscript received October 30, 2018; revised May 8, 2019; accepted May 9, 2019. Date of publication June 18, 2019; date of current version August 9, 2019. The review of this paper was arranged by Senior Editor H. B. Garrett. *(Corresponding author: Andreas Waets.)*

A. Waets and F. Cipriani are with the Space Environments and Effects Section (TEC-EPS), European Space Agency, 2201 AZ Noordwijk, The Netherlands (e-mail: andreas.waets@esa.int; fabrice.cipriani@esa.int).

S. Ranvier is with the Division of Space Physics, Royal Belgian Institute for Space Aeronomy (BIRA-IASB), 1180 Brussels, Belgium (e-mail: sylvain.ranvier@aeronomie.be).

Color versions of one or more of the figures in this paper are available online at http://ieeexplore.ieee.org.

Digital Object Identifier 10.1109/TPS.2019.2920136

The LEO plasma environment is generally considered to be benign concerning spacecraft charging risks [4], except in the auroral regions. At the altitude of PICASSO, the spacecraft velocity is said to be *mesothermal*, i.e., it is faster than the ion thermal velocity but lower than the electron thermal velocity

$$v_i < v_{S/C} < v_e \tag{1}$$

with the particle thermal velocity equal to $v_{e,i} = (2\ kT_{e,i}/m)^{1/2}$. In this regime, the spacecraft will produce a wake when moving through the plasma: the low ion velocity causes a depleted ion region directly downstream of the spacecraft [5]. As a consequence, the potentials on dielectric surfaces in the plasma wake will tend to be negative with respect to the plasma in eclipse because electrons have larger mobility than ions and the majority of ions can only access the ram spacecraft side. The wake side is also depleted of electrons, due to the negative potential resulting from the space charge of those electrons that are present. However, the electron thermal velocity ensures that negative charges can reach all surfaces. The low plasma energy and large plasma density in LEO keep the surface potentials on the spacecraft to be limited, remaining between a few tenths of volts negative and up to a few volts positive when the spacecraft is illuminated by sunlight [6].

The high inclination (98°) of PICASSO's orbit will cause the spacecraft to periodically cross the cusps in the earth's magnetosphere where high-energy auroral electrons can be encountered. These precipitating high-temperature (>10 keV) electron fluxes seem to correspond with ion depletion regions ($<10^{10}$ m^{-3}) [4], and in this environment, spacecraft has been observed to charge to a highly negative potential (several kilovolts) as reported, e.g., for the Defence Meteorological Satellite Program (DMSP) spacecraft in [7]. When the spacecraft surface is made of materials with different conductivities, especially dielectrics, there is a risk of severe differential charging triggering electrostatic discharges. Due to the similar orbit as DMSP and the presence of dielectric surface materials on PICASSO, we have assessed the effect of the auroral plasma environment on the spacecraft.

III. PICASSO Spacecraft and SLP Instrument

The PICASSO spacecraft has the dimensions of a generic 3U cubesat platform (340.5 mm × 100 mm × 100 mm) featuring four deployable panels, acting as solar arrays [1]. The spacecraft (S/C) itself is covered in a conductive gold layer, and the back side of the solar panels is made of a nonconductive epoxylike layer. The solar cells are covered with glass, which is also nonconductive. A 3-D CAD rendering of PICASSO is shown in Fig. 1.

The SLP instrument consists of four individual cylindrical Langmuir probes mounted on the extremities of the solar panels to ensure that at least one probe is out of the S/C wake at all times [3]. The probes are 40-mm-long Ti tubes of 2-mm diameter, connected to the solar panel via a 40-mm-long boom. In nominal mode, SLP sweeps the potential of the probes from −5 to +13 V with respect to the S/C floating potential while the collected current by the probes is measured to extract an IV characteristic. For sufficiently negative potentials, electrons are repelled and only ions are attracted, and the probes measure the ion saturation current from which the ion density can be retrieved. On the contrary for positive potentials, the probes collect the electron saturation current from which the electron density can be extracted. The electron temperature and the S/C potential are retrieved from the electron retardation region, where the potential of the probes is close to that of the plasma so that both ions and electrons are attracted [8].

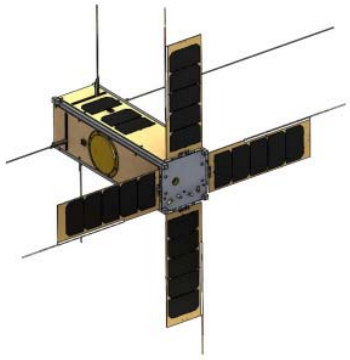

Fig. 1. CAD rendering of the PICASSO cubesat illustrating deployed solar panels and mounted Langmuir probes on the edges.

The issue with operating Langmuir probes on a cubesat is the limited amount of conducting collecting surfaces: when the probes are swept with a positive bias, the S/C will consequently charge negatively to achieve a neutral current balance. This charging will lead to a drift of the S/C potential during the sweep, making the data unstable and unusable. There is also the risk that the potential of the S/C drops so much that the probes cannot be biased to measure properly in the electron saturation region. To circumvent this problem, a technique using two probes is used: one probe is biased to measure the collected current, while another probe only measures the spacecraft floating potential. This way, the consistent I–V characteristics can be retrieved. To ensure that the probes can sweep properly in the electron saturation region all along the orbit, the conducting surface of the S/C has been increased to have at least 200 cm^2 on all sides of the S/C.

IV. SPIS Simulations and Results

The LEO plasma that PICASSO will encounter is relatively benign toward spacecraft charging effects since it is composed of cold and high-density plasma [4]. In any space plasma, the spacecraft acts as a Langmuir probe, which potential will float to a surface potential determined by an equilibrium current balance. In a nondrifting plasma with a Maxwellian temperature distribution, a surface typically charges to about three times the electron temperature [9], which, considering the environment parameters given in Table I, is generally several tenths of a volt negative. The high density and the mesothermal S/C velocity lead to high current densities, which makes high surface potentials impossible [5]. In cold plasma, the perturbation caused by potential is also more effectively screened from the surroundings and stays limited to a region

TABLE II
SPIS SIMULATION ENVIRONMENT PARAMETERS

	electrons	ions (O^+)
Temperature k_BT [eV]	0.2	0.2
Density [m^{-3}]	10^{10}	10^{10}
Population type	Maxwell-Boltzmann	PIC
S/C velocity [m/s]	7500	
Simulation time [s]	20	

known as the sheath. The typical length scale of a sheath is the Debye length

$$\lambda_D = \sqrt{\frac{\epsilon_0 k_B T}{e^2 n}} \tag{2}$$

where ϵ_0 is the permittivity of the vacuum, k_BT is the particle's thermal energy, n is the plasma density, and e is the elementary charge. Since the Debye length is small, the spacecraft is large compared with the size of the sheath even for small-sized cubesats. The distribution of charges needs to be considered as a continuum instead of a collection of distinct pointlike charges requiring the spacecraft-plasma interaction problem to be solved using Poisson's equation

$$\nabla^2 \Phi = -\frac{\rho}{\epsilon_0} \tag{3}$$

where Φ is the scalar potential and ρ is the space charge density [10]. Solving (3) can be done numerically using the particle-in-cell (PIC) method, which requires the proper definition of a mesh. PIC codes such as SPIS require the resolution of the mesh elements to be less than half of the Debye length to produce physical results, making LEO simulations a numerically heavy and in most cases unfeasible task. However, the limited size of PICASSO and the associated simulation volume enable us to use a PIC model to simulate spacecraft charging. A description of the baseline simulation environment parameters is given in Table II.

A plasma environment with equal electron and ion temperature (0.2 eV) and density (1.0×10^{10} m^{-3}) was chosen as a representative case for PICASSO. This value is on the lower end of the density range detailed in Table I but was chosen to yield reasonable computation times and physical results in SPIS. A typical LEO orbital velocity (7500 m/s) was converted to an equivalent ion drift velocity flowing in the opposite direction of the spacecraft. The implementation of this drift velocity was necessary to reproduce the wake effect and requires the use of a PIC population for the ions, which are assumed to be solely composed of oxygen atoms (O^+). A fluid approximation is used for electrons represented by the Maxwell–Boltzmann distribution. The collected electrons currents are computed using an Orbital Motion Limited (OML) approximation, which can results in up to 20% error when considering very positive potentials ($\sim$10 V) at the positive end of the LP sweep range [11]. A new collection scheme is being implemented in the code to overcome such limitations and was not ready at the time of this paper. The plasma is considered to be collisionless and unmagnetized. In the LEO environment,

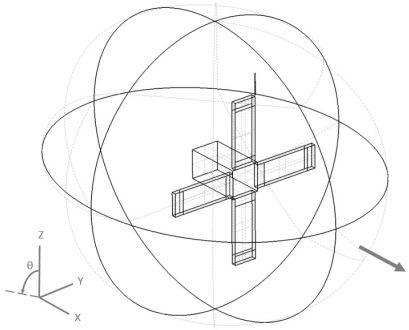

Fig. 2. Geometrical model of PICASSO inside an ellipsoidal computational volume used for the PIC simulations, including one LP on the $+Z$-oriented solar panel. The spacecraft velocity was fixed along the positive x-axis (indicated by the gray arrow), and the rotation of the spacecraft is defined around the y-axis as the angle between the positive z-axis (fixed) and the axis going through the LP. The actual S/C attitude during operation will not be maintained as represented here, and this configuration was only chosen as a baseline for simulations.

PICASSO will encounter, and the electron gyroradius is less than 10 cm and for ions several meters [4]. The magnetization can be estimated by calculating the ratio of the respective gyroradii to the typical length scale, resulting in a weakly magnetized plasma for electrons and unmagnetized plasma for ions. The decision to not take into account magnetic field effects was made for computational purposes, and its possible consequences will be further discussed in Section V.

The environment detailed in Table II corresponds to a Debye length of 3 cm, smaller than the length scale of PICASSO itself but much larger than, e.g., the Langmuir probe radius (1 mm). The mesh resolution was chosen on all parts of the spacecraft and in the simulation volume to be 1 cm in order to meet the Debye length criterion. The S/C geometry respects the exact dimensions and surface areas of PICASSO including the requirement of having a 200 cm^2 collecting area on each side. The simulation geometrical model is shown in Fig. 2. The materials used for the spacecraft surfaces were gold (including the LP), cover glass for the solar cells (only on the $+X$-oriented side of the S/C), and epoxy for the back side of the solar panels. The different material groups are connected through a simplified electrical circuit without voltage bias between the groups themselves, allowing each group to float freely with respect to each other.

A. LEO Charging Environment

The surface potential evolution in eclipse for the different parts of PICASSO in the simulated environment (see Table II) is shown in Fig. 3. Due to the absence of photoemission currents, all potentials are negative with the S/C ground equilibrating at -0.725 V. The dielectric material on the back side of the solar arrays charges to roughly -2 V. An LP sweep was programmed to start at 10 s and includes 20 fixed-bias voltage steps between -5 and 13 V (PICASSO's operating limits). Measurements of the collected electron and ion currents were taken with a delay after each voltage step to ensure the stabilization of the surface potentials, and in this way, the impact of biasing the Langmuir probes was assessed. From

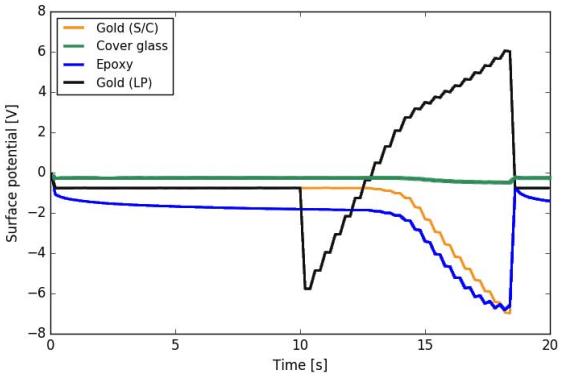

Fig. 3. Surface potentials in eclipse as a function of time for the four electrical nodes in the S/C simulation model. The surface potentials for all materials are contained between 0 and −2 V in equilibrium. The effect of the LP sweep voltage stepping can be seen in the potential evolution on all nodes, most prominently on the S/C ground and epoxy surface potential. Due to the effect of the bias voltage with respect to the S/C ground, the slope of the sweep steps is reduced, reaching a maximum of roughly 6 V positive and limiting the electron saturation regime measurement range.

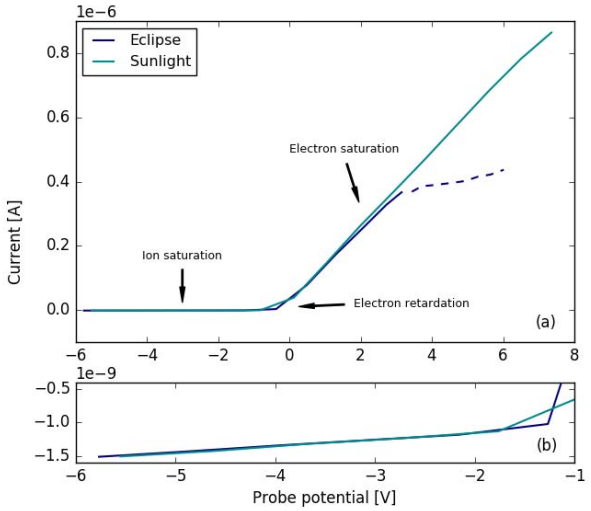

Fig. 4. (a) I–V characteristics extracted from LP sweeps in eclipse and sunlight detailing the different regions of interest. The limitations of executing an LP sweep on a cubesat can be seen from the shape of the eclipse I–V characteristic: data points are intelligible up to +3-V probe voltage as opposed to +8 V in the sunlit case, resulting from the limited amount of current that can be drawn from the plasma. (b) More detailed view of the ion saturation current that is negative in the I–V characteristic by convention [8].

probe voltages of +3 V and upward, the slope of the voltage stepping decreases due to the negative bias of the S/C ground potential. The maximum voltage of the probe with respect to the plasma is only roughly +6 V as opposed to the +13-V operating limit. As a consequence, the IV characteristic shows that the collected current is falling off at +3 V, resulting in biased data points beyond this limit (as shown in Fig. 4). This effect is caused by the collected electron current on the probe, which cannot exceed the ram ion current on the spacecraft surface, necessary to establish a current balance.

For comparison, a simulation in sunlight was carried out. The photoemission currents slightly increase the equilibrium potentials of the surfaces, but the biggest effect is seen during the LP sweep itself: as a result of negative charge being carried away from the surface due to photoemission, the S/C electrical ground is driven down less than in eclipse. The LP voltage can, therefore, reach +10 V with usable data points up to +8 V, as shown in Fig. 4(a). The effect of photoemission on the resulting I–V characteristic extracted from the LP was not analyzed here. For higher plasma densities ($>10^{10}$ m^{-3}), the photoemission is expected to play a less important role since the ram ion current accounts for the majority of positive current to the spacecraft.

The effect of the solar arrays in the spacecraft circuit has been omitted in this paper but has been reported to pose an issue when collecting electrons for positive probe bias voltages during the LP sweep. On PICASSO, a string of five cells with exposed interconnects and metalized back faces can reach a maximum voltage of 15 V at the end of the array in a cold LEO plasma. The positive bias of solar arrays and exposed interconnects when in sunlight can drive the spacecraft's floating potential down since they draw a larger negative current from the plasma, which can be compensated by the ram ions and photoemission (both contributing positive charge to the current balance) [12]. By consequence, this also drives the LP voltage with respect to the plasma down and inhibits the proper collection of the electron saturation current, which is further discussed in the following. Up to now, simulations of the PICASSO circuit and LP operation did not include the (biased) solar arrays, having that 200-cm^2 conductive surface on each side of the spacecraft was deemed sufficient to ensure a proper biasing of the Langmuir probe [3]. This paper was carried out during the integration of the satellite, but future studies should address the current collection by the exposed solar array elements and its effects on the S/C floating potential during a sweep.

B. Effect of Spacecraft Rotation

The analysis of the PICASSO surface charging and LP operation explained in IV-A was carried out for a fixed orientation in which the S/C body was aligned parallel to the velocity vector, the solar arrays, and the Langmuir probe oriented perpendicular to the velocity vector. To investigate more realistic spacecraft attitudes, this analysis can be extended toward different angles of orientation, altering the currents on the LP. The angles are defined between the positive x-axis and the axis going through the LP, as shown in Fig. 2. The effect of the orientation on the I–V characteristics and the extracted parameters is reported in this section by detailing the behavior in the three different I–V characteristic regions separately: the ion saturation region, the electron retardation region, and the electron saturation region.

1) Ion Saturation Region: The ion saturation current is likely to be affected the most by the orientation of the S/C. Given the fact that the S/C velocity is mesothermal, the LP will only collect the ram ion current, i.e., only ions flowing in a surface area projected along the S/C velocity vector will reach the LP and a cosine modulation of collected current is expected. Moreover, when the probe is in the wake, one also expects to see a decrease due to the depletion of the ion density. These effects are shown in Fig. 5, which shows

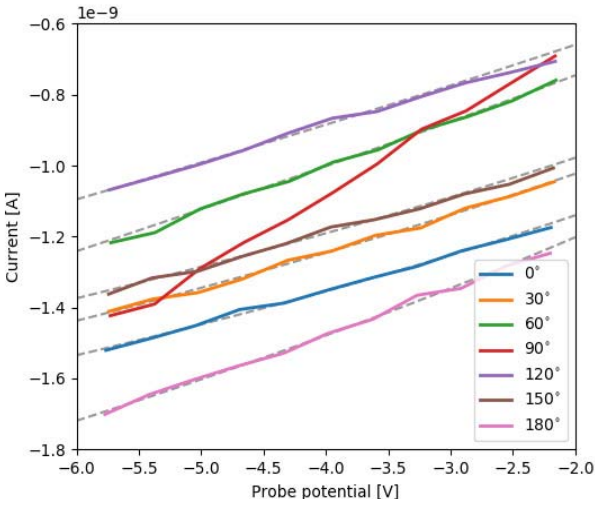

Fig. 5. Ion saturation currents as a function of probe potential for angles between the +z axis and the LP (as defined in Fig. 2). Comparing angles 0°, 30°, and 60° shows a reduction in collected current since, for larger angles, the LP collects the ram current over a smaller area. The lowest amount of collected current corresponds to the 120° case where the probe is in the wake of the S/C. All saturation currents show more or less the same behavior except for the 90° (when the LP is oriented parallel to S/C velocity) case. Even though 0° and 180° correspond to the same orientation with respect to the S/C velocity, there is a significant difference. The dashed lines indicate the fitted curves according to (5) used to extract the ion density.

the ion saturation regions for angles between 0° and 180° in steps of 30°. The largest currents are observed in the 0° and 180° cases, corresponding to the maximum possible collecting surface area of the probe. Increasing the angle from 0° upward, indeed, sees a reduction in the current with the 120° case as a minimum since, here, the probe is located in the wake of the spacecraft, as shown in Fig. 6. The 90° case shows a significantly different behavior than the rest of the curves, collecting a very small current near 0-V probe potential but increasing more rapidly toward more negative voltages.

In order to quantify these effects, the ion saturation currents were fitted using a theoretical model. The effective area over which the probe collects charges is determined by the sheath thickness R_s, which depends on the probe potential. In the ion saturation regime, the probe potential Φ is much larger than the plasma temperature $k_B T \ll e\Phi$, allowing us to approximate the sheath thickness as [13]

$$R_s = \lambda_D \sqrt{\frac{2e\Phi}{k_B T}} \tag{4}$$

in terms of the Debye length, given by (2). The ion saturation current is measured for voltages roughly between -5 and -2 V, giving the sheath thickness a minimum value of around 15 cm. In this regime, the current collected by the LP can be estimated using the OML theory as developed by Mott-Smith and Langmuir [14] in a thick sheath environment [9] since $R_s/R_p \gg 1$. A generalization of the OML current to spherical and cylindrical probes in the limit of high drift velocity plasmas was made by Hoegy and Wharton [15], given by

$$I_i \approx -eN_i A v_{S/C} \left(1 + \frac{k_B T_i}{m v_{S/C}^2} + \frac{2e\Phi}{m v_{S/C}^2}\right)^d \tag{5}$$

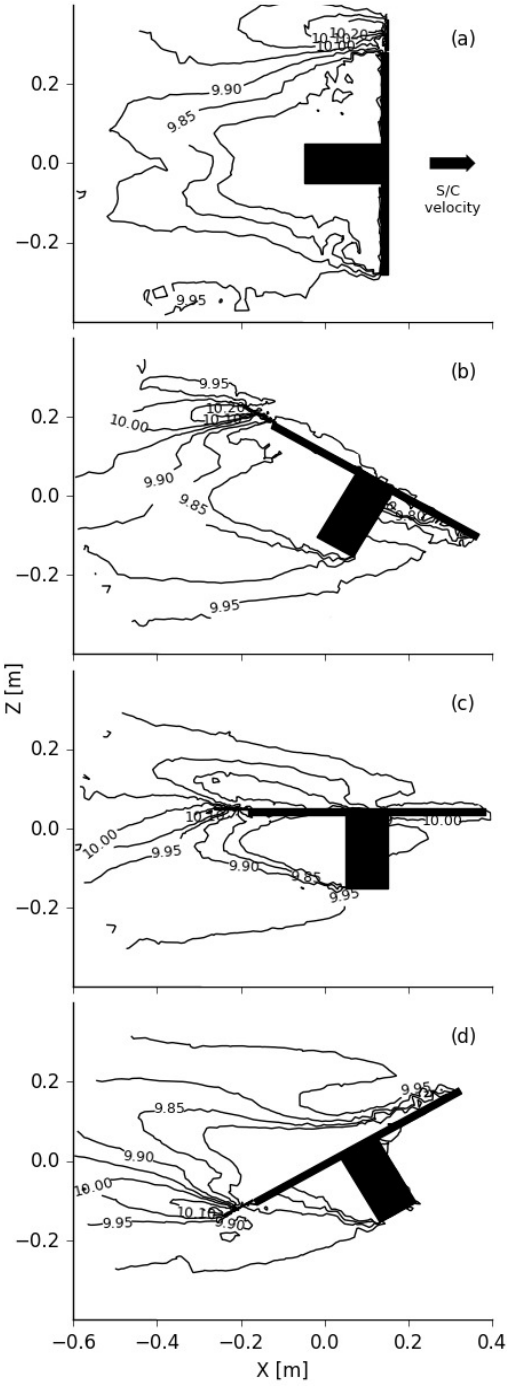

Fig. 6. Contour plots of the ion density in logarithmic scale around the PICASSO spacecraft extracted from SPIS simulations for angles (a) 0°, (b) 60°, (c) 90°, and (d) 120° in the xz plane. The density profiles were all extracted after 12 s of simulations at which point the Langmuir probes were biased at roughly -1.5 V with respect to the S/C ground, explaining the local density increase on the wake side of the LP. A density depletion is clearly seen on the wake side of the spacecraft but is limited to within 10% near the LP.

where N_i is the ion density, m_i is the (O^+) ion mass, and $A = 2R_p l \cos(\theta)$ is the probe area projected along the S/C velocity $v_{S/C}$. The exponent d equals 1/2 or 1 for cylindrical or spherical probes, respectively. Note that, by convention, the collected ion current to a Langmuir probe is considered to be negative, whereas the electron current is considered to

TABLE III
ION SATURATION CURRENT FIT PARAMETERS

Angle [°]	N_i $[m^{-3}]$	d [ ]
0	9.47×10^9	0.632
30	9.50×10^9	0.723
60	1.06×10^{10}	1.081
90	–	–
120	1.89×10^{10}	1.062
150	9.12×10^9	7.874
180	9.54×10^9	7.600

be positive [8]. This approximation is valid for Mach numbers (the ratio between the spacecraft velocity with respect to the stationary plasma and the ion thermal velocity) larger than 2.5. In the LEO plasma environment, the Mach number is ~ 8 [4], and hence, this expression can be used to fit the simulated data points in the ion saturation region using a least-squares method. The density N_i is a free parameter, ignoring the negligible current contribution from the electron population, as well as the exponent d to account for any effects coming from the fact that the probe is not an ideal, infinite cylinder but connected to the spacecraft and the large sheath size with respect to the probe radius. The results of the fitting procedure for angles between 0° and 180° are listed in Table III.

The ion density values extracted from the fit slightly underestimate but all lie within a 10% range from the imposed simulation plasma density of 1×10^{10} m^{-3} except for the 120° case. Here, the probe is in the wake of the S/C where the density of ions is depleted but this effect is not observed, and on the contrary, it accounts for the largest estimated ion density. Using (5), a fit with reasonable results for the 90° data was not obtained due to the parallel orientation of the LP to the S/C velocity. As reported in [3], the LP measuring plasma data will be out of the wake, and hence, the results for the 90° and 120° cases are of limited importance for operation onboard PICASSO. The values for the exponent d deviate from the expected value of $1/2$ for cylindrical probes significantly and even reach spherical probe collection for angles 60° and 120°. The deviation can be explained by the large sheath size with respect to the probe radius for probe voltages in the ion saturation current regime and the end effects of the LP not being taken into account as described in [16]. This point is further addressed in Section V.

2) Electron Retardation Region: When the bias potential is close to the plasma potential, the measured current is the sum of the electron and ion current. The electron retardation current [16]

$$I_e \propto \exp\left(\frac{e\Phi}{k_B T_e}\right) \tag{6}$$

can be used to obtain the electron temperature T_e and is independent of geometry. The simulated data can be fitted as a function of the probe potential Φ, which was done for the 0° and 60° cases and shown in Fig. 7. For comparison, the electron retardation current to a free-floating LP of 40-mm length and 1-mm radius is also shown, illustrating that this

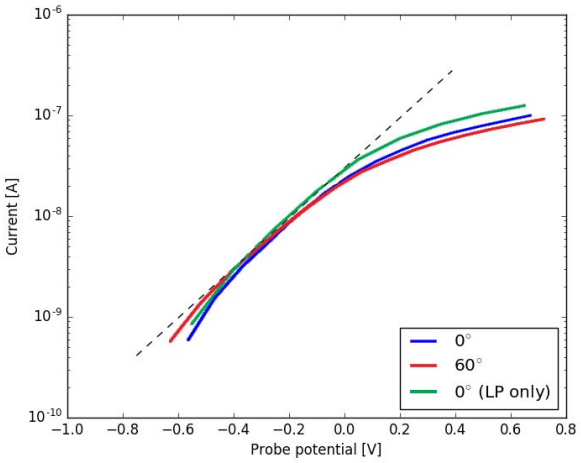

Fig. 7. Logarithm of the collected current as a function of probe potential in the electron retardation region, shown for the 0° and 60° cases and compared with the characteristic obtained by simulating only the LP without spacecraft. These data points were fitted with a straight line (dashed curve) to extract the electron temperature. The retardation region is largely unaffected by the S/C geometry or orientation.

TABLE IV
EXTRACTED PARAMETERS FROM THE ELECTRON RETARDATION REGION

Angle [°]	$k_B T_e$ $[eV]$	Φ_p $[V]$	$\Phi_{S/C}$ $[V]$
0 [a]	0.199	0.306	-0.673
0	0.207	0.148	-0.655
60	0.207	0.132	-0.767

[a] Simulation for LP only with l = 0.04 m

region of the I–V characteristic is, indeed, not affected by geometry but as can be seen also not by the angle of rotation with respect to the S/C velocity. Electrons are the dominant collected species, whereas the ions constitute only a minor portion of the collected current. The calculated electron temperatures extracted from the simulated data are listed in Table IV. This portion of the characteristic was sampled at a higher frequency to achieve adequate time resolution, in a similar way as will be done for the actual SLP instrument on-board PICASSO [3].

The lower edge of the electron retardation region is defined by the S/C floating potential [16] at which a zero net current on the spacecraft is achieved. This was obtained by interpolating the data points just below and above the zero current point. The extracted values approximate the simulated S/C ground potential (approximately -0.725 V). On the other edge of the retardation region, the "knee" in the curve determines the plasma potential. Fitting the data points in the retardation region and the saturation region separately and determining the crossing define this inflection point. Small positive values lower than 0.5 V for the plasma potential are found, corresponding to the imposed 0-V plasma potential. The calculated values for the S/C floating potential $\Phi_{S/C}$ and the plasma potential Φ_p for the characteristics shown in Fig. 7 are also listed in Table IV.

3) Electron Saturation Region: For sufficiently positive probe potentials, the ion current to the probe becomes

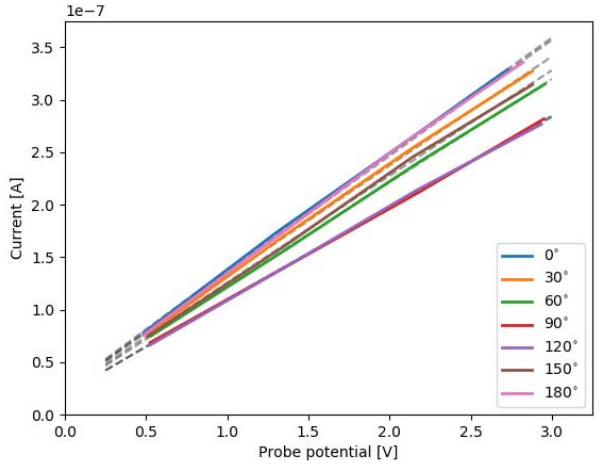

Fig. 8. Electron saturation currents as a function of probe potential. A little variation as a result of orientation is seen with the exception of 90° and 120°, which collect significantly less current.

negligible, and the electron saturation current is collected. In the mesothermal S/C velocity regime, the thermal velocity of the electrons is such that we can assume the current to be isotropic to both the spacecraft and the Langmuir probe. Any effects from S/C rotation can be neglected. This is seen in Fig. 8, where the electron saturation currents are plotted for angles of rotation between 0° and 180°. The currents show not much variation as expected but we can see that the 90° and 120° orientations correspond to significantly lower collected current than the other angles. Using a similar procedure as for the ion saturation current, we can quantify these effects by fitting the data points to a theoretical model. The electron saturation current as a function of probe potential Φ can be approximated by [17]

$$I_e \approx eN_eA\sqrt{\frac{k_BT_e}{2\pi m_e}}\left(1+\frac{e\Phi}{k_BT_e}\right)^d \tag{7}$$

where N_e is the electron density, m_e is the electron mass, k_BT_e is the electron temperature, $A = 2\pi R_p l$ is the LP collecting surface area now taken to be equal to the total cylinder surface (without ends), and the exponent d equals to $1/2$ or 1 for cylindrical or spherical collection, respectively. This expression was fitted to the simulated data points using the electron density N_e and exponent d as fit parameters with the electron temperature assumed to be known and fixed at 0.2 eV. The results of the least-squares fitting procedure are listed in Table V. The obtained densities underestimate imposed plasma density by at least 20%. In the extracted data, there also appears to be a modulation as a function of angle with respect to the S/C velocity vector: the lowest obtained densities correspond to the LP located in the wake.

A possible explanation for this could be that the electron density in the wake is depleted since the ambipolar diffusion will occur at a slower rate due to the lower ion density [18]. Density maps of the electron population extracted from SPIS confirmed that the density of electrons can drop to 30% in the most depleted wake region. The fitting procedure allows to obtain exponent values very close to 1, showing a clear

TABLE V
ELECTRON SATURATION CURRENT FIT PARAMETERS

Angle [°]	N_e [m^{-3}]	d [ ]
0	8.01×10^9	0.976
30	7.76×10^9	0.969
60	7.03×10^9	0.981
90	6.38×10^9	0.974
120	6.44×10^9	0.969
150	7.32×10^9	0.976
180	7.72×10^9	0.987

tendency toward a spherical probe collection law rather than a cylindrical law. In addition, the effects of having a probe of finite length and connection to a larger body can explain the inconsistencies in the obtained values. This is further discussed in Section V.

C. Charging in Auroral Environment

As already stated in Section II, the high inclination of PICASSO's orbit will make it pass the auroral regions where the spacecraft will encounter much different plasma parameters than the ones used up to now for analyzing the S/C charging of PICASSO and the performance of the SLP instrument. As reported from observations made by the DMSP spacecraft [7], the surface potential can drop down to several kilovolts negative. The necessary conditions for charging appear to be a thermal plasma density less than 10^{10} m^{-3}, a high integral precipitating electron number flux (>10^8 cm^2 s^{-1} sr^{-1}) for energies greater than 14 keV, and most of the charging events happened in eclipse. Charging of large objects (such as DMSP) in LEO polar orbits has been studied extensively, and analytical models were developed (see [19]), but the charging risks on cubesat platforms remain fairly unknown. To study this, an auroral environment was implemented based on the European Cooperation for Space Standardization worst case charging distribution [20], which is derived from DMSP observations. A Maxwellian fit to the distribution was made, resulting in an electron population of temperature 11 keV and density equal to 1×10^7 m^{-3}. This population is not the most adequate to describe an auroral environment but was chosen for computational reasons. The low ambient plasma density requirement for high-voltage charging is not strictly defined since the detectors on DMSP were unable to sample plasma densities below 10^{10} m^{-3}, hence the background density associated with precipitating high-energy electron fluxes is unknown. The auroral environment is described in Table VI, the background plasma density was chosen to be 10^8, 10^9, and 10^{10} m^{-3}, respectively, for both electrons and ions. The temperature was kept at 0.2 eV and the S/C velocity was fixed at 7500 m/s as defined in Table II, and all simulations were performed in eclipse. For simulation stability, the LP was not included in the geometry here.

The results are shown in Fig. 9 for a total simulation time of 20 s. The hierarchy of surface potentials is the same as for the baseline LEO simulation case, as shown in Fig. 3: the cover glass surface charging the most positive and the epoxy the

TABLE VI
AURORA SIMULATION ENVIRONMENT PARAMETERS

	ions (O^+)	electrons (ambient)	electrons (aurora)
Temperature k_BT [eV]	0.2	0.2	11×10^3
Density [m^{-3}]	$10^8 - 10^{10}$	$10^8 - 10^{10}$	10^7
Population type	PIC	Maxwell-Boltzmann	Maxwell-Boltzmann
S/C velocity [m/s]	7500		
Simulation time [s]	20		

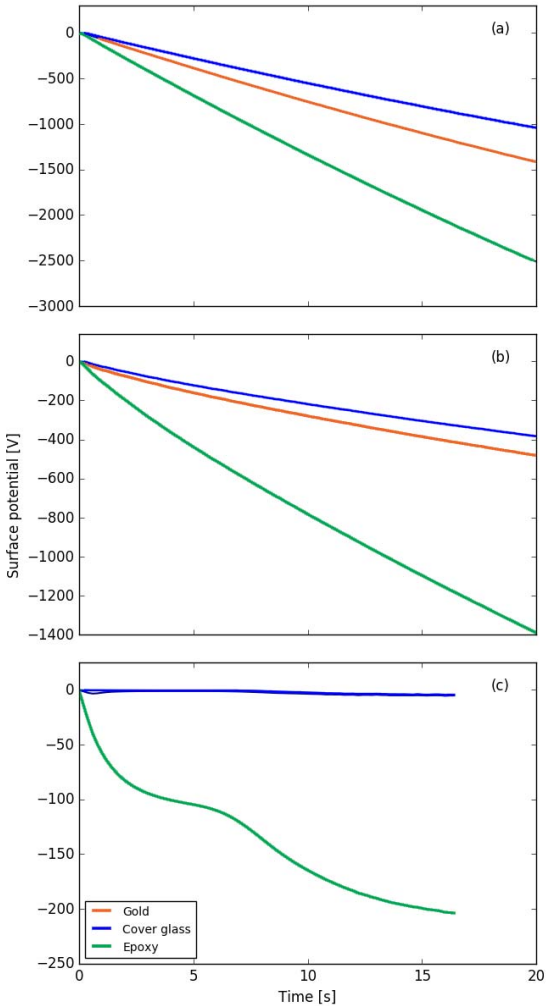

Fig. 9. Potentials of PICASSO surface materials as a function of time in an auroral environment with background density (a) 10^8, (b) 10^9, and (c) 10^{10} m^{-3}. Significant differential charging develops for all cases, and absolute charging levels increase for decreasing background densities.

most negative due to its location on the S/C wake side with the gold acting as the S/C ground in between. For a background density of 10^8 m^{-3}, the cover glass and the gold surfaces reach several hundreds of volt negative, while the epoxy surface charges down to -2500 V within the simulation time span. Increasing the background density to 10^9 m^{-3} shows that the surface potentials decrease markedly as expected since the surface can attract more positive current from the ambient plasma. The surface potentials do not reach an equilibrium value within 20 s, and from the trend of the curves, it is possible that this will not happen in a time span of minutes. In both 10^8 m^{-3} and 10^9 m^{-3} background density cases, the ion density and current collecting surface on the satellite is so small, and the conducting spacecraft surface (acting as electrical ground) keeps charging negatively in absolute levels. A large portion of the S/C surface is covered in a dielectric material having a large capacitance with respect to the ground. The absolute S/C capacitance (with respect to the plasma at infinity) is composed of the relative capacitances between the dielectric surfaces and the S/C ground proportionally to their respective areas. Treating the surface as a collection of coupled electrical nodes in contact with the plasma, the charging time associated with this coupled capacitance can also be very long [21]. The environment in these cases bears resemblance to a geosynchronous satellite in geomagnetic storm conditions, where enduring periods of frame charging have been observed [22]. It is, however, unlikely that PICASSO will encounter this particular worst case environment for such a long time. As identified on the DMSP spacecraft, the charging events can be associated with the so-called inverted-V regions in visible auroral arcs [7]. Most of the events were of the order of seconds; the average was 8 s. However, under the right circumstances orbital and magnetic field configuration, the spacecraft can experience an auroral arc pass of 2 m. This constitutes about the longest that an LEO satellite can be expected to charge during an auroral crossing [6]. When imposing a background plasma density of 10^{10} m^{-3}, we can see that the charging of cover glass and gold material surface potentials remains limited, reaching down to roughly -5 V and the charging is fast. The charging of the epoxy surface material shows a peculiar time evolution due to the complex wake morphology forming behind the PICASSO simulation model. As can be seen from ion density maps, an ion focusing region develops on the wake side of the S/C model from which a positive current can flow to the epoxy surfaces, which varies as a function of the epoxy surface potential. We can see that the potential will likely equilibrate around -200 V, and the time evolution was cut off due to a simulation instability.

As mentioned before, the LP was not included for the simulations in the auroral environment. We can, however, infer that due to the significant surface charging, the LP will not be able to reach the bias voltages needed for sampling the different I–V characteristic regions properly.

V. DISCUSSION

Simulating spacecraft-plasma interactions in LEO is a difficult task due to the heavy numerical load and long computation times needed. SPIS, the software tool used for this paper, can simulate this type of interaction by relying on 3-D PIC methods. The time integration process of simulation requires the careful setting of the different numerical time steps before initializing the kernel. To optimize the integration scheme, the numerical time steps can be chosen to differ from the physical time steps as was done in this paper. This can greatly decrease the needed simulation time but care must be taken that the simulation results remain physical. An optimized

parameter set was found for the baseline plasma environment specified in Table II but required a number of modifications on the PICASSO geometry, such as increasing the thickness of the solar panels to ensure stable simulations.

To reduce the computation time, the simulated LP sweeps consisted of maximum 20 bias voltage steps between PICASSO's limit operating voltages (−5 and 13 V) or dedicated ranges to sample the ion saturation current or the electron retardation region. The biasing of the Langmuir probe causes a drift of the spacecraft ground potential, which is not necessarily a physical effect. In this paper, we chose to set the equilibration time between the voltage steps to 0.4 s, much longer than the fixed sampling frequency of 10 kHz intended for SLP [3]. For this frequency, the potentials may not have time to equilibrate, and the drift of the spacecraft ground can be less severe. The effect of spacecraft ground potential drift due to the biasing can only be properly assessed when a representative electrical circuit is implied. A dedicated simulation also incorporating a more realistic spacecraft circuit (including biased solar arrays) is needed to fully understand the effects of sweeping the probe in the desired voltage ranges. As discussed in [12], large current drops have been observed when the spacecraft is in sunlight with solar arrays switched ON. If the outcome of the simulations shows that the probes cannot be biased to sample the electron saturation current, the solar arrays can be grounded by the positive end to only expose negative potentials to the spacecraft or coated to keep them from drawing a negative current from the plasma.

Extracting the plasma parameters by fitting theoretical probe models needed to be done by using a limited amount of data points subject to fluctuations in the simulated plasma. Therefore, the effects on the I–V characteristic caused by the PICASSO spacecraft itself are obscured. Despite this, the imposed ion densities are retrieved from the fits with reasonable accuracy for most obtained I–V sweep curves, generally underestimating by 10% using a spherical current collection law on a cylindrical surface. The electron densities are consistently underestimated by at least 20% using this fitting procedure. There is a room for improvement here by more thoroughly analyzing the effect of the finite-length cylindrical probe and the spacecraft itself as an obstacle. As described in [16], the estimated electron density can differ considerably due to finite length and end effects. The value of the exponent in the collection law [as defined in (5) and (7)] for the ion saturation current deviates from $1/2$ but the electron saturation current fits better using an exponent close to 1, resembling a more spherical probe collection profile. A similar observation for simulated cylindrical Langmuir probes was made in [23] with fitted exponents between 0.7 and 0.8, and thereby, also noting deviations from using an OML type of current collection law is prone to inaccuracies as a consequence of the size and geometry of the probe with respect to the Debye length. In this sense, a parameterization of the OML current to the probe is desirable to ensure the correct interpretation of the data from the SLP instrument on PICASSO by using a semiempirical law, as was demonstrated in [24]. For this, the system can be benchmarked in a plasma chamber, and in a similar way, the effect of the S/C rotation on the current collection can be investigated and verified on the ground. Knowing the S/C and LP orientation with respect to the stationary plasma is necessary to obtain intelligible data as reported in [25], which describes a cubesat mission carrying a double LP, similar to the PICASSO's SLP instrument. In addition, a magnetic field can be included to study its effect as was done in [26].

As already stated previously, the plasma seen by the Langmuir probe can be considered weakly magnetized (for electrons) and unmagnetized (for ions). However, the magnetic field is expected to have an effect on the collected current for electrons because when there is no magnetic field, the electrons come from all directions, whereas when there is a magnetic field, the electrons are confined to a magnetic flux tube of radius equivalent to the electron thermal gyroradius. Therefore, the collected electron current is expected to be lower when imposing a magnetic field. As reported in [27], the orientation of the magnetic field is expected to have a very limited effect for small probes.

A number of modifications to the implementation of the auroral environment are possible to yield more realistic results. In this paper, the high-energy auroral electrons were modeled as an isotropic Maxwellian distribution fitted to a worst case charging electron spectrum. In contrast, electron distributions associated with high-level charging events are highly non-isotropic and directed along the magnetic field lines [4]. These features were not feasible to simulate in SPIS, and their effects could, therefore, not be studied.

VI. Conclusion

The surface charging of PICASSO and the operation of the SLP were analyzed using the spacecraft-plasma interaction tool, SPIS. In the expected plasma environment, the surface materials charge to several volts negative. Theoretical probe collection laws were used to extract the implemented plasma environment parameters by fitting the simulated data points for several spacecraft orientations. For the extraction of plasma parameters from the on-board data, the S/C attitude could be monitored to take into account its effect on the I–V sweep curve. The plasma density and the temperature were extracted with reasonable accuracy, as well as the plasma and spacecraft potential. The spacecraft surface materials are shown to exhibit substantial absolute and differential charging in a worst case auroral environment reaching several hundreds or even thousands of volts negative, in accordance with observations from polar orbit spacecraft.

References

[1] B. Mero *et al.*, "PICASSO: A state of the art cubesat," in *Proc. AIAA/USU Conf. Small Satell.*, 2015. [Online]. Available: http://digitalcommons.usu.edu/smallsat/2015/all2015/15/

[2] B. Thiébault, J.-C. M. Velez, J. Forest, and P. Sarrailh. *Spis 5.1 Online Documentation*. Accessed: Feb. 1, 2017. [Online]. Available: http://dev.spis.org/static/documentation/

[3] S. Ranvier *et al.*, "Use of a Langmuir probe instrument on board a Pico-satellite," *IEEE Trans. Plasma Sci.*, vol. 45, no. 8, pp. 2007–2012, Aug. 2017.

[4] D. E. Hastings, "A review of plasma interactions with spacecraft in low earth orbit," *J. Geophys. Res., Space Phys.*, vol. 100, no. A8, pp. 14457–14483. [Online]. Available: https://agupubs.onlinelibrary.wiley.com/doi/abs/10.1029/94JA03358

[5] E. J. Daly and D. J. Rodgers, *Plasma Interactions at Low Altitudes*, R. N. Dewitt, D. Duston, and A. K. Hyder, Eds. Dordrecht, The Netherlands: Springer, 1993.

[6] P. C. Anderson, "Characteristics of spacecraft charging in low earth orbit," *J. Geophys. Res., Space Phys.*, vol. 117, no. A7, 2012, Art. no. A07308. doi: 10.1029/2011JA016875.

[7] H.-C. Yeh and M. S. Gussenhoven, "The statistical electron environment for defense meteorological satellite program eclipse charging," *J. Geophys. Res., Space Phys.*, vol. 92, no. A7, pp. 7705–7715, 1987. [Online]. Available: https://agupubs.onlinelibrary.wiley.com/doi/abs/10.1029/JA092iA07p07705

[8] R. L. Merlino, "Understanding Langmuir probe current-voltage characteristics," *Amer. J. Phys.*, vol. 75, no. 12, pp. 1078–1085, 2007. doi: 10.1119/1.2772282.

[9] S. Lai, *Fundamentals of Spacecraft Charging: Spacecraft Interactions With Space Plasmas*. Princeton, NJ, USA: Princeton Univ. Press, 2011.

[10] D. J. Griffiths, *Introduction to Electrodynamics*, 4th ed. Boston, MA, USA: Cambridge Univ. Press, 2017. [Online]. Available: https://cds.cern.ch/record/1492149

[11] O. J. Ferro, S. Hess, E. Seran, C. Bastien-Thiry, and D. Payan, "Coupled fluid-kinetic numerical method to model spacecraft charging in Leo," *IEEE Trans. Plasma Sci.*, vol. 46, no. 3, pp. 651–658, Mar. 2018.

[12] L. H. Brace, "Langmuir probe measurements in the ionosphere," in *American Geophysical Union Geophysical Monograph Series*. Washington, DC, USA: American Geophysical Union, 1998, p. 23.

[13] M. A. Lieberman, *Direct Current (DC) Sheaths*. Hoboken, NJ, USA: Wiley, 2005, ch. 6, pp. 165–206. [Online]. Available: https://onlinelibrary.wiley.com/doi/abs/10.1002/0471724254.ch6

[14] H. M. Mott-Smith and I. Langmuir, "The theory of collectors in gaseous discharges," *Phys. Rev. J. Arch.*, vol. 28, pp. 727–763, Oct. 1926. [Online]. Available: https://link.aps.org/doi/10.1103/PhysRev.28.727

[15] W. R. Hoegy and L. E. Wharton, "Current to a moving cylindrical electrostatic probe," *J. Appl. Phys.*, vol. 44, p. 5365, Jan. 1974.

[16] R. L. Boggess, L. H. Brace, and N. W. Spencer, "Langmuir probe measurements in the ionosphere," *J. Geophys. Res.*, vol. 64, no. 10, pp. 1627–1630, 1959. doi: 10.1029/JZ064i010p01627.

[17] F. F. Chen, J. D. Evans, W. Zawalski, J. D. Evans, and W. Zawalski, "Electric probes," in *Plasma Diagnostic Techniques*, R. H. Huddlestone and S. L. Leornard, Eds. New York, NY, USA: Academic, 1965.

[18] R. M. Albarran and A. Barjatya, "Plasma density analysis of cubesat wakes in the earth's ionosphere," *J. Spacecraft Rockets*, vol. 53, pp. 393–400, Apr. 2016.

[19] D. E. Parks and I. Katz, "Charging of a large object in low polar earth orbit," in *Spacecraft Design, Testing and Performance* (Spacecraft Charging Technology). San Diego, CA, USA: NASA, 1980, pp. 979–989.

[20] ESA. (2008). *ECSS-E-ST-10-04C Space Environment Standard*. [Online]. Available: https://www.spacewx.com/Docs/ECSS-E-ST-10-04C_15Nov2008.pdf

[21] H. B. Garrett, "The charging of spacecraft surfaces," *Rev. Geophys.*, vol. 19, no. 4, pp. 577–616, 1981. [Online]. Available: https://agupubs.onlinelibrary.wiley.com/doi/abs/10.1029/RG019i004p00577

[22] J.-C. Matéo-Vélez, A. Sicard, D. Payan, N. Ganushkina, N. P. Meredith, and I. Sillanpää, "Spacecraft surface charging induced by severe environments at geosynchronous orbit," *Space Weather*, vol. 16, no. 1, pp. 89–106, 2018. [Online]. Available: https://agupubs.onlinelibrary.wiley.com/doi/abs/10.1002/2017SW001689

[23] R. Marchand, S. Marholm, D. Darian, W. Miloch, and M. Mortensen, "Impact of miniaturized fixed-bias multi-needle Langmuir probes on cubesats," in *Proc. 15th SCTC*, Kobe, Japan, 2018, pp. 1–9.

[24] A. R. Hoskinson and N. Hershkowitz, "Effect of finite length on the current–voltage characteristic of a cylindrical Langmuir probe in a multidipole plasma chamber," *Plasma Sources Sci. Technol.*, vol. 15, no. 1, pp. 85–90, Jan. 2006. doi: 10.1088%2F0963-0252%2F15%2F1%2F013.

[25] T. R. Tejumola, G. W. Z. Segura, S. Kim, A. Khan, and M. Cho, "Validation of double Langmuir probe in-orbit performance onboard a nano-satellite," *Acta Astron.*, vol. 144, pp. 388–396, Mar. 2018. [Online]. Available: http://www.sciencedirect.com/science/article/pii/S0094576517311803

[26] P. A. R. Lira and R. Marchand, "Simulations of non-ideal effects in Langmuir Probe Measurements," in *Proc. 15th SCTC*, Kobe, Japan, 2018.

[27] N. Imtiaz, R. Marchand, and J.-P. Lebreton, "Modeling of current characteristics of segmented Langmuir probe on DEMETER," *Phys. Plasmas*, vol. 20, no. 5, 2012, Art. no. 052903.